J. Acoust. Soc. Jpn. (*E*) **17**, 2 (1996)

Detection of nonlinearly propagating focused sound emitted from uniform source using a concave receiver

Shigemi Saito

Faculty of Marine Science and Technology, Tokai University, 3-20-1, Orido, Shimizu, 424 Japan

(*Received 26 July 1995*)

The property of the fundamental and second harmonic components of the acoustic pressure in the beam emitted from a uniformly excited focusing source, which is detected by a concave receiver put normal to the acoustic axis beyond the focal region, has been investigated for both the cases of the free field and the field with inserted sample. Calculation based on the successive approximation solution for the Khokhlov-Zabolotskaya-Kuznetsov equation is validated through experiments. It has been clarified that the range dependence of the fundamental component amplitude differs from that of the second harmonic, unlike the case of a Gaussian source, and the cancellation of the second harmonic components generated in front of and beyond the focal region is degraded comparing with the case of Gaussian source. The signal experimentally received beyond the sample corresponds fairly well with the theoretical prediction, taking into account the acoustic properties of the inserted sample. However, the result of experimental determination of the B/A utilizing such responses shows slightly poorer agreement with the literature values, due to the less sensitive property of the second harmonic component to the inserted sample.

Keywords: Nonlinear acoustics, Focused ultrasound, Second harmonic, Acoustic microscope, Nonlinearity parameter, Finite amplitude method

PACS number: 43. 25. Cb, 43. 25. Zx, 43. 25. Jh, 43. 80. Ev, 43. 35. Sx

1. INTRODUCTION

The present author and his colleagues have analyzed the nonlinearly generated second harmonic component in a focused sound including the problems of its spatial distribution.[1-6] On the other hand, acoustic microscopes have recently been applied to various ultrasonic measurements, where focused ultrasounds are employed to obtain the high spatial resolution of an acoustic imaging and a wide variety of incidence angles on a sample. Although the nonlinear propagation of the ultrasonic wave must take place in the acoustic microscope, the phenomenon has rarely been used for the measurement so far.

The acoustic nonlinearity parameter B/A, which describes the relative magnitude of the quadratic term of density dependence of acoustic pressure in the medium, is an important acoustic property for evaluating the waveform distortion and nonlinear attenuation in the medium. In addition, it has been suggested that this parameter, B/A, is useful for characterizing materials including biological tissues, so the B/A measurement is also of great interest. In order to develop the B/A measurement method utilizing acoustic microscopes for the final goal, the present author has proposed the B/A measurement using focused ultrasound based on the finite amplitude method,[7] where the B/A is obtained through observing the second harmonic component contained in the acoustic pressure after passing through the sample.[8,9] This method employs a focusing Gaussian source whose vibrational amplitude distribution is weighted in Gaussian function such that a diffraction induced by the source edge can be neglected. The field analysis is then significantly facilitated, and the variance and uncertainty of observed values caused by the complicated acoustic field can be avoided. However, since an acoustic microscope usually does not employ the Gaussian source, this measurement cannot be immediately applied to the microscope.

In the present paper, assuming a uniformly excited concave source as a more realistic source for acoustic microscopes, the fundamental and second harmonic components of the focused acoustic field observed with another concave receiver are theoretically and experimentally examined. In measuring the B/A, the influence of a sample inserted within the focal region on the acoustic field beyond the sample will be utilized. Here the acoustic waves detected by the concave receiver for both the cases with and without insertion of the sample are investigated. The analytical result is examined from the view point of the possibility to measure the nonlinearity parameter B/A of the inserted sample. The experimental determination of the B/A for a few samples are also conducted.

2. FREE FIELD DETECTED BY CONCAVE RECEIVER

Suppose that a uniformly excited concave source with a focal length D and radius a emanates a sinusoidal sound of angular frequency ω along the z axis as shown in Fig. 1. The focused sound is detected by a concave receiver whose curvature and aperture radii are d and b, respectively. Taking into consideration the harmonic components up to the second order, the acoustic pressure at the point (r, z) is assumed to be $p_1(r, z)\exp(-j\omega\tau)+p_2(r, z)\cdot\exp(-j2\omega\tau)$. Here τ is the retarded time $t-z/c_w$,

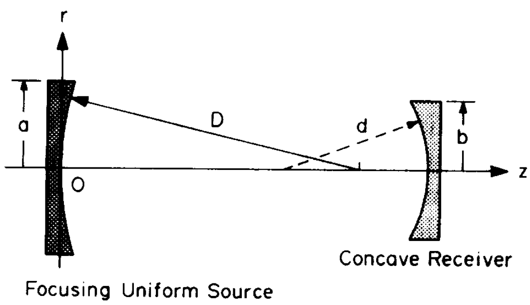

Fig. 1 Geometry and notation.

where t is the time, and c_w is the sound speed in water. Then the fundamental and second harmonic components in the output voltage of the concave receiver are approximately proportional to the integrations of pressure over the receiver surface

$$P_1(z)=\int_0^b p_1(r, z)\exp\left(-j\frac{k_w r^2}{2d}\right)rdr, \quad (1)$$

$$P_2(z)=\int_0^b p_2(r, z)\exp\left(-j\frac{k_w r^2}{d}\right)rdr, \quad (2)$$

where k_w is the wavenumber of the fundamental in water ω/c_w. Since the above proportion factors of the output signals to P_1 and P_2, which should depend primarily on the receiver sensitivity, are not significant in the discussion that follows, the output voltage is assumed to be $P=P_1\exp(-j\omega\tau)+P_2\exp(-j2\omega\tau)$ for simplicity. The sound field formed by a concave source with a relatively small aperture angle is well described by the Khokhlov-Zabolotskaya-Kuznetsov equation, which is the parabolic approximation of the wave equation taking into account nonlinear propagation as well as linear attenuation.[10] The successive approximation solution of the KZK equation for a free field without any insertion of sample is

$$p_{1w}(r, z)=-j\frac{k_w p_0}{z}\exp\left(j\frac{k_w r^2}{2z}\right)\exp(-\alpha_w z)\cdot\int_0^a J_0\left(\frac{k_w rx}{z}\right)\exp\left[j\frac{k_w x^2}{2}\left(\frac{1}{z}-\frac{1}{D}\right)\right]xdx, \quad (3)$$

$$p_{2w}(r, z)=j\frac{\beta_w k_w{}^3 p_0{}^2}{2\pi\rho_w c_w{}^2 z}\exp(-4\alpha_w z)\exp\left(j\frac{k_w r^2}{z}\right)\cdot\int_{\theta=0}^{\pi}\int_{x=0}^{a}\int_{y=0}^{a}\int_{z'=0}^{z}\frac{\exp(2\alpha_w z')}{z'}\cdot\exp\left(j\frac{G}{z'}\right)\exp\left[-j\frac{k_w}{2D}(x^2+y^2)\right]\cdot\exp\left(j\frac{k_w F}{4z}\right)\cdot J_0\left(\frac{k_w r}{z}\sqrt{F}\right)xydz'dydxd\theta, \quad (4)$$

where p_0, ρ_w, α_w and β_w are the on-source pressure, the density of water, the attenuation coefficient in water at the fundamental frequency, and the acoustic nonlinearity parameter $1+(B/A)_w/2$ of water. Further, $J_0(\cdot)$ is the Bessel function of 0-th order, $F=x^2+y^2-2xy\cos\theta$, and $G=k_w(x^2+y^2+2xy\cdot\cos\theta)/4$. Substituting Eqs. (3) and (4) into Eqs. (1) and (2) respectively, one derives the fundamental component P_{1w} and the second harmonic component P_{2w} contained in the output voltage of the receiver for the case without insertion of the sample:

$$P_{1\mathrm{w}}(z)=-j\frac{k_\mathrm{w}p_0}{z}\int_{r=0}^{b}\int_{x=0}^{a}\exp\left[j\frac{k_\mathrm{w}r^2}{2}\left(\frac{1}{z}-\frac{1}{d}\right)+j\frac{k_\mathrm{w}x^2}{2}\left(\frac{1}{z}-\frac{1}{D}\right)\right]J_0\left(\frac{k_\mathrm{w}rx}{z}\right)rxdxdr\,, \quad (5)$$

$$P_{2\mathrm{w}}(z)=j\frac{\beta_\mathrm{w}k_\mathrm{w}^3p_0^2}{2\pi\rho_\mathrm{w}c_\mathrm{w}^2z}\int_{r=0}^{b}\int_{\theta=0}^{\pi}\int_{x=0}^{a}\int_{y=0}^{a}E_1\left(-j\frac{G}{z}\right)\cdot\exp\left(-j\frac{G}{z}\right)\exp\left[j\,k_\mathrm{w}r^2\left(\frac{1}{z}-\frac{1}{d}\right)+j\frac{k_\mathrm{w}(x^2+y^2)}{2}\left(\frac{1}{z}-\frac{1}{D}\right)\right]\cdot J_0\left(\frac{k_\mathrm{w}r}{z}\sqrt{F}\right)rxydydxd\theta dr\,. \quad (6)$$

Here $\alpha_\mathrm{w}=0$ has been assumed for simplicity, so the formula

$$\int_0^z\frac{1}{z'+a}\exp\left(\frac{jb}{z'+a}\right)dz'=E_1\left(-j\frac{b}{z+a}\right)-E_1\left(-j\frac{b}{a}\right) \quad (7)$$

was available for the integration by z' in Eq. (4), where $E_1(\cdot)$ is the exponential integral function defined as

$$E_1(-jx)=\int_x^\infty\frac{\exp(jt)}{t}dt\,.$$

When the aperture radius of the receiver is large compared to the beam width, the use of an integral formula

$$\int_0^\infty x\exp(jax^2)J_0(bx)dx=\frac{j}{2a}\exp\left(-j\frac{b^2}{4a}\right),$$

which is applicable to Eqs. (5) and (6) when the infinitely large b is assumed, reduces $P_{1\mathrm{w}}(z)$ and $P_{2\mathrm{w}}(z)$ of Eqs. (3) and (4) as follows:

$$P_{1\mathrm{w}}(z)=\frac{jp_0}{1-z/d}\frac{1-\exp\left[j\frac{k_\mathrm{w}a^2}{2}\left\{\frac{1}{z}-\frac{1}{D}-\frac{1}{z(1-z/d)}\right\}\right]}{k_\mathrm{w}\left\{\frac{1}{z}-\frac{1}{D}-\frac{1}{z(1-z/d)}\right\}}, \quad (8)$$

$$P_{2\mathrm{w}}(z)=-\frac{\beta_\mathrm{w}k_\mathrm{w}^2p_0^2}{4\pi\rho_\mathrm{w}c_\mathrm{w}^2(1-z/d)}\int_{\theta=0}^{\pi}\int_{x=0}^{a}\int_{y=0}^{a}E_1\left(-j\frac{G}{z}\right)\exp\left(-j\frac{G}{z}\right)\cdot\exp\left[-j\frac{k_\mathrm{w}F}{4z(1-z/d)}+j\frac{k_\mathrm{w}(x^2+y^2)}{2}\left(\frac{1}{z}-\frac{1}{D}\right)\right]xydydxd\theta\,. \quad (9)$$

The sound beam of the frequency $f=1.9$ MHz emitted from a uniformly excited focusing source of the aperture radius $a=23.5$ mm and the focal length $D=85$ mm was experimentally observed with a concave receiver set as shown in Fig. 1. The receiver consists of a PZT transducer with the thickness dilatational resonance frequency of 4 MHz, whose aperture and curvature radii are $b=20$ mm and $d=42$ mm, respectively. The amplitudes of the fundamental and second harmonic components of the receiver output experimentally observed at various distances from the source at 20°C water temperature are shown by the hollow circles in Figs. 2(a) and 2(b). They coincide well with the solid curves calculated from Eqs. (5) and (6). The acoustic property of water at 20°C was employed for the calculation; $\rho_\mathrm{w}=1000$ kg/m^3, $c_\mathrm{w}=1483$ m/s, $\alpha_\mathrm{w}=0.11$ Np/m, and $(B/A)_\mathrm{w}=5.0$. The dotted curves show the values calculated more simply with Eqs. (8) and (9) assuming an infinitely large b. Since the experimental receiver is large enough to detect the whole beam, the dotted curves almost coincide with the solid curves. For the second harmonic sound of narrower beam, the dotted curve completely coincides with the solid curve. Comparing Fig. 2(a) with Fig. 2(b), it is seen that the z dependence of the fundamental greatly differs from that of the second harmonic. This is different from the property of a Gaussian source, in which they show almost the same z-dependence as each other. However it is common to the case of a Gaussian source that they attain the maximum amplitudes in the vicinity of $z=D+d$, that is $z=127$ mm in the present experiment. It is supposed that the acoustic pressure within the whole beam has the identical phase on the receiver surface at this location. The phase parameter which defines the phase delay of the second harmonic component relative to the fundamental, Φ_w, is shown in Fig. 2(c). Large errors may be contained in the measured phase parameter because of extremely frequency dependent sensitivity of the experimental receiver with the resonance frequency at 4 MHz, to which the frequency of the second harmonic sound is close. Nevertheless the

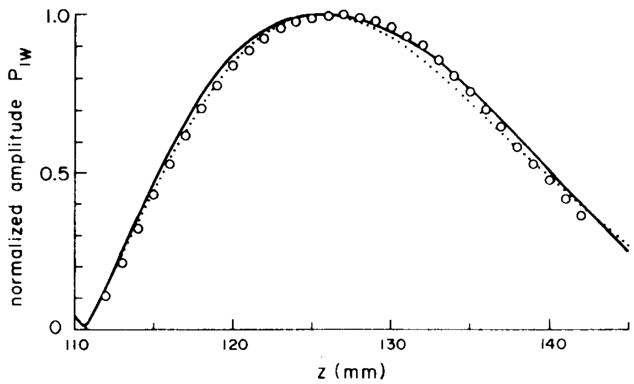

(a) Fundamental amplitude.

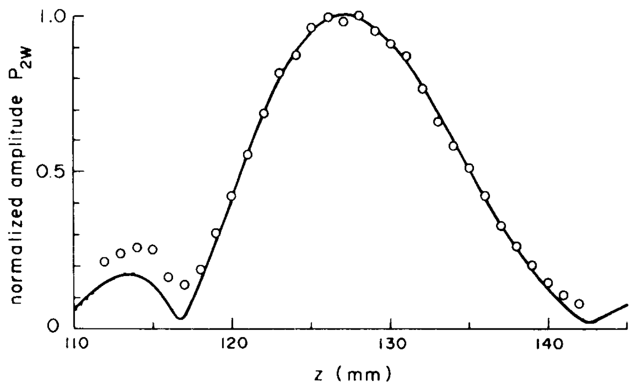

(b) Second harmonic amplitude.

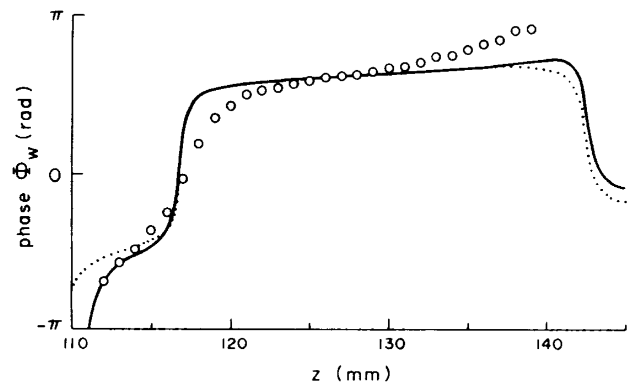

(c) Phase parameter.

Fig. 2 Range dependence of signal obtained with a concave receiver.

measured result agrees well with the calculated one near $z=D+d$. The measurement error must be, therefore, rather small.

3. FIELD WITH DIFFERENT LIQUID LAYER

Suppose that a different liquid layer of the thickness L is set vertical to the axis. The density, sound speed, and acoustic nonlinearity parameter in the layer are denoted by ρ, c, and $\beta=1+(B/A)/2$, respectively. The attenuation coefficient in the liquid layer is assumed to be α_1 at the fundamental frequency and α_2 at the second harmonic frequency. Then the fundamental acoustic pressure $p_{1s}(r, z)$ and the second harmonic acoustic pressure $p_{2s}(r, z)$ are given as follows:[11]

$$P_{1s}(r,z)=-j\frac{T_{11}T_{01}k_w}{z_a}p_0\exp[-\{\alpha_w(z-L)+\alpha_1L\}]\cdot\exp\left(j\frac{k_w}{2z_a}r^2\right)\int_0^a\exp\left[j\frac{k_wx^2}{2}\left(\frac{1}{z_a}-\frac{1}{D}\right)\right]\cdot J_0\left(\frac{k_wr}{z_a}x\right)dx\,, \qquad (10)$$

$$\begin{aligned}P_{2s}(r,z)=&\,j\frac{k_w^3p_0^2}{2\pi\rho_wc_w^2z_a}\exp[-4\alpha_w(z-L)-\alpha_2L]\\&\cdot\exp\left(j\frac{k_wr^2}{z_a}\right)\int_{\theta=0}^{\pi}\int_{x=0}^{a}\int_{y=0}^{a}\Bigg\{\beta_wT_{12}T_{02}\\&\cdot\int_{z'=0}^{z_1}\frac{\exp(2\alpha_wz')}{z'}\exp\left(j\frac{G}{z'}\right)dz'\\&+\beta T_{11}^2T_{02}\frac{\rho_wc_w^3}{\rho c^3}\exp(2\alpha_wz_1)\\&\cdot\int_{z'=0}^{L}\frac{\exp[(\alpha_2-2\alpha_1)z']}{z_1+cz'/c_w}\\&\cdot\exp\left(\frac{jG}{z_1+cz'/c_w}\right)dz'+\beta_wT_{11}^2T_{01}^2\\&\cdot\exp[2\alpha_wz_1+(\alpha_2-2\alpha_1)L]\\&\cdot\int_{z'=0}^{z-z_0}\frac{\exp(2\alpha_wz')}{z'+z_1+cL/c_w}\\&\cdot\exp\left(\frac{jG}{z'+z_1+cL/c_w}\right)dz'\Bigg\}\\&\cdot\exp\left[-j\frac{k_w}{2D}(x^2+y^2)\right]\exp\left(j\frac{k_wF}{4z_a}\right)\\&\cdot J_0\left(\frac{k_wr}{z_a}\sqrt{F}\right)xydydxd\theta\,,\end{aligned} \qquad (11)$$

where $z_a=z+(c/c_w-1)L$. Here z_1 and z_0 are the z coordinates at the acoustic wave inlet and outlet of the liquid layer, respectively, namely $z_0-z_1=L$. The pressure transmission coefficients at $z=z_1$ and z_0 have been regarded identical to the transmission coefficients T_{1n} and T_{0n} for a planar wave, where n is the order of higher harmonics. Integrating p_{1s} and p_{2s} over the surface of the concave receiver as expressed in Eqs. (1) and (2), the fundamental and second harmonic components of the output voltage of the concave receiver are derived as follows:

$$P_{1s}(z)=-j\frac{T_{11}T_{01}k_w}{z_a}p_0\exp[-\{\alpha_w(z-L)+\alpha_1L\}]\cdot\int_{r=0}^{b}\int_{x=0}^{a}\exp\left[j\frac{k_w}{2}\left\{\left(\frac{1}{z_a}-\frac{1}{D}\right)x^2\right.\right.$$

$$+\left(\frac{1}{z_a}-\frac{1}{d}\right)r^2\Big\}\Big]J_0\left(\frac{k_w r}{z_a}x\right)rxdxdr\,, \tag{12}$$

$$P_{2s}(z)=j\frac{k_w^3 p_0^2}{2\pi\rho_w c_w^2 z_a}\exp\left[-4\alpha_w(z-L)-\alpha_2 L\right]$$
$$\cdot\int_{r=0}^{b}\int_{\theta=0}^{\pi}\int_{x=0}^{a}\int_{y=0}^{a}\exp\left[jk_w\left(\frac{1}{z_a}-\frac{1}{d}\right)r^2\right]$$
$$\cdot\left\{\beta_w T_{12}T_{02}\int_{z'=0}^{z_1}\frac{\exp(2\alpha_w z')}{z'}\exp\left(j\frac{G}{z'}\right)dz'\right.$$
$$+\beta T_{11}^2 T_{02}\frac{\rho_w c_w^3}{\rho c^3}\exp(2\alpha_w z_1)$$
$$\cdot\int_{z'=0}^{L}\frac{\exp[(\alpha_2-2\alpha_1)z']}{z_1+cz'/c_w}\exp\left(\frac{jG}{z_1+cz'/c_w}\right)dz'$$
$$+\beta_w T_{11}^2 T_{01}^2\exp[2\alpha_w z_1+(\alpha_2-2\alpha_1)L]$$
$$\cdot\int_{z'=0}^{z-z_0}\frac{\exp(2\alpha_w z')}{z'+z_1+cL/c_w}$$
$$\left.\cdot\exp\left(\frac{jG}{z'+z_1+cL/c_w}\right)dz'\right\}$$
$$\cdot\exp\left[-j\frac{k_w}{2D}(x^2+y^2)\right]$$
$$\cdot\exp\left(j\frac{k_w F}{4z_a}\right)J_0\left(\frac{k_w r}{z_a}\sqrt{F}\right)rxydydxd\theta dr\,. \tag{13}$$

When the receiver aperture is large, the approximation of infinite b makes Eqs. (12) and (13) reduce to

$$P_{1s}(z)=j\frac{T_{11}T_{01}p_0\exp[-\{\alpha_w(z-L)+\alpha_1 L\}]}{1-z_a/d}$$
$$\cdot\frac{1-\exp\left[j\frac{k_w a^2}{2}\left\{\frac{1}{z_a}-\frac{1}{D}-\frac{1}{z_a(1-z_a/d)}\right\}\right]}{k_w\left\{\frac{1}{z_a}-\frac{1}{D}-\frac{1}{z_a(1-z_a/d)}\right\}}\,, \tag{14}$$

$$P_{2s}(z)=-\frac{k_w^2 p_0^2}{4\pi\rho_w c_w^2 z_a\left(\frac{1}{z_a}-\frac{1}{d}\right)}$$
$$\cdot\exp[-4\alpha_w(z-L)-\alpha_2 L]$$
$$\cdot\int_{\theta=0}^{\pi}\int_{x=0}^{a}\int_{y=0}^{a}\left\{\beta_w T_{12}T_{02}\right.$$
$$\cdot\int_{z'=0}^{z_1}\frac{\exp(2\alpha_w z')}{z'}\exp\left(j\frac{G}{z'}\right)dz'$$
$$+\beta T_{11}^2 T_{02}\frac{\rho_w c_w^3}{\rho c^3}\exp(2\alpha_w z_1)$$
$$\cdot\int_{z'=0}^{L}\frac{\exp[(\alpha_2-2\alpha_1)z']}{z_1+cz'/c_w}\exp\left(\frac{jG}{z_1+cz'/c_w}\right)dz'$$
$$+\beta_w T_{11}^2 T_{01}^2\exp[2\alpha_w z_1+(\alpha_2-2\alpha_1)L]$$
$$\cdot\int_{z'=0}^{z-z_0}\frac{\exp(2\alpha_w z')}{z'+z_1+cL/c_w}$$
$$\left.\cdot\exp\left(\frac{jG}{z'+z_1+cL/c_w}\right)dz'\right\}$$
$$\cdot\exp\left[-j\frac{k_w}{2D}(x^2+y^2)\right]$$
$$\cdot\exp\left[j\frac{k_w F}{4}\left\{\frac{1}{z_a}-\frac{1}{z_a(1-z_a/d)}\right\}\right]xydydxd\theta\,. \tag{15}$$

When $\alpha_w=0$, the integration by z' in the first and third terms of Eqs. (13) and (15) is simplified using Eq. (7). Further, when the attenuation in the liquid layer is small, putting $\exp\{(\alpha_2-2\alpha_1)z'\}=1$ simplifies the integration of second term in the same way. Comparing Eq. (5) with Eq. (12), or Eq. (8) with Eq. (14), it is seen that z in the former equations has been replaced with z_a in the latter equations, excepting the range dependence factor of attenuation. If the range for the maximum amplitude in the case of free field is defined as $z=z_w$, the maximum amplitude in the case with a different liquid layer is attained at $z=z_w-(c/c_w-1)L$, since the range dependence due to the attenuation is not effective. This shift of the maximum range is due to the refraction at the interface between water and the different liquid. The refraction has been taken into account in the derivation of Eqs. (10) and (11) under the continuity conditions for acoustic pressure and normal particle velocity at the interface.[11] The range where the maximum amplitude is obtained in the case with different liquid layer is named z_s here.

Putting a layer of methanol of thickness $L=20$ mm such that its center locates at $z=D$, the experiment has been carried out. The experimental results of the range dependence of the amplitudes of the fundamental signal P_{1s} and second harmonic signal P_{2s} are shown in Fig. 3 as well as that of the phase parameter Φ_s. The measured result shows a good agreement with the theoretical prediction shown by the solid curves calculated using Eqs. (12) and (13). The dotted curves in the figures show the computation using Eqs. (14) and (15). The acoustic property of $\rho=797$ kg/m^3, $c=1{,}121$ m/s, $\alpha_1=\alpha_2=0$, and $B/A=9.6$ was assumed for methanol in the calculation. It is explained by the aforementioned equation $z_s=z_w-(c/c_w-1)L$ that the range for the maximum fundamental amplitude shifts far from the source by 5 mm due to the difference between methanol and water in the sound speed.

The fundamental amplitude, second harmonic amplitude, and phase parameter at each maximum amplitude range for the case with and without the methanol layer are compared in Figs. 4(a) and 4(b) at various source pressures. The experimental

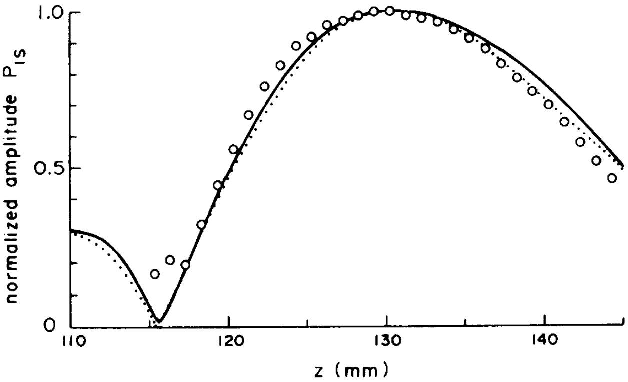

(a) Fundamental amplitude.

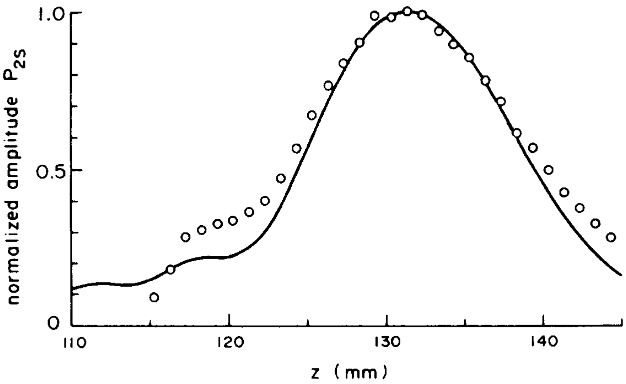

(b) Second harmonic amplitude.

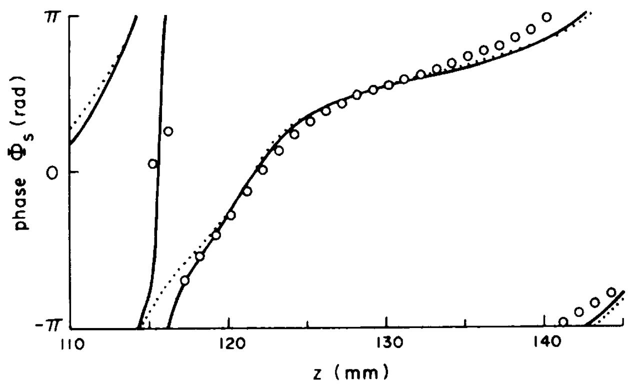

(c) Phase parameter.

Fig. 3 Range dependence of signal received beyond a methanol sample.

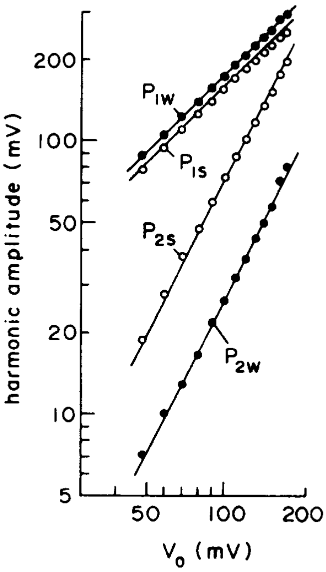

(a) Harmonic amplitude.

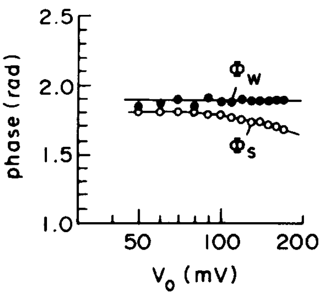

(b) Phase parameter.

Fig. 4 Comparison of amplitudes and phases for cases with and without insertion of methanol sample.

results for the case without and with the sample are shown by the symbol ● and ○, respectively. The solid curve connects the experimental values. The abscissa indicates the voltage V_0 of the input signal to the power amplifier to drive the source, to which the source pressure is proportional. The experimental result shows that the insertion of the methanol layer reduces the fundamental amplitude 0.92 times, and magnifies the second harmonic amplitude 2.7 times. In addition, the experimental data show 0.09 rad decrease of the phase parameter after insertion of the sample within a small amplitude range, where the successive approximation is applicable. The aforementioned calculation predicts the effects of 0.94 times decrease in fundamental amplitude, 2.64 times increase in second harmonic amplitude, and 0.04 rad reduction in phase parameter. The experimental result shows a fairly good agreement with the calculated.

4. COMPARISON WITH GAUSSIAN SOURCE

In the case of a Gaussian source, the nonlinearity parameter B/A of the inserted sample can be measured utilizing a detected signal at the receiver position, where the maximum amplitude is obtained.[9]

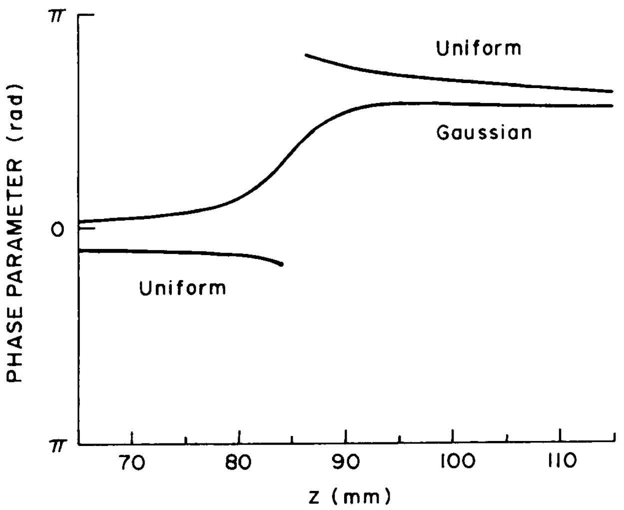

Fig. 5 Phase parameters at maximum amplitude position for uniform and Gaussian focusing sources.

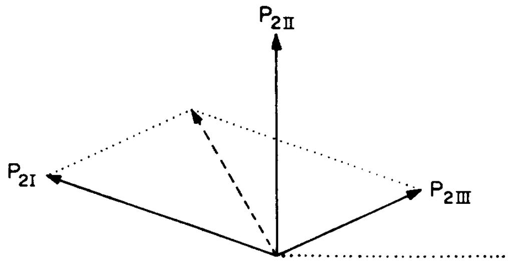

(a) Uniform focusing source.

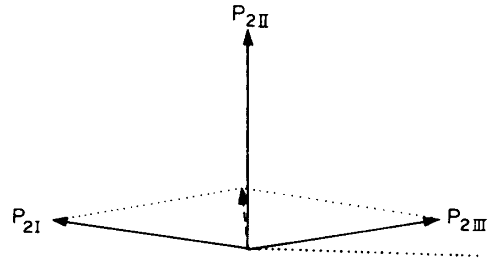

(b) Gaussian focusing source.

Fig. 6 Vector diagram for second harmonic components.

The detected signal at such a distance is supposed to be important also in the case of the uniform source. The signal property of this position is compared with that for the Gaussian source. The range for the maximum amplitude depends on the curvature radius d of the receiver. The Φ_w calculated at the range $z=D+d$, to which the maximum-amplitude position is very close, is shown in Fig. 5. In this calculation, the receiver curvature radius of $d=z-D$ has been assumed for each distance z. At $z<D$, therefore, the receiver must be a convex one with negative d. Further, the approximation using an infinitely large value of b was employed for simplicity. In the figure, the phase parameters for the case of a Gaussian source with a Gaussian distribution coefficient of $\xi=2{,}300\ \mathrm{m}^{-2}$ and the same concavity as the experimental uniform source is also shown for the purpose of comparison. The Φ_w for both sources greatly varies as the acoustic wave passes through the focal region. The meanings of these variances look identical, but they differ from each other in detail as discussed below.

Here the focused acoustic field is divided in three parts; the regions of $z<D-s$, $D-s<z<D+s$, and $z>D+s$, which are named region I, II, and III, respectively. The second harmonic component of the signal detected beyond the focal region is assumed to be the summation of the second harmonic signals, $P_{2\mathrm{I}}$, $P_{2\mathrm{II}}$, and $P_{2\mathrm{III}}$, which are generated during the passage through the regions I, II, and III before the observation position, respectively. Assuming that the acoustic property of the inserted sample is the same as that of water, the first, second, and third terms of Eq. (15) give $P_{2\mathrm{I}}$, $P_{2\mathrm{II}}$, and $P_{2\mathrm{III}}$, respectively. Figure 6(a) illustrates the complex amplitudes of $P_{2\mathrm{I}}$, $P_{2\mathrm{II}}$, and $P_{2\mathrm{III}}$ at the range $z=2D$ calculated for the experimental source with another receiver of $d=D$, assuming $s=10$ mm. Figure 6(b) shows those calculated using Eq. (14) of Ref. 6 for the similarly detected signal when a Gaussian source with a Gaussian distribution coefficient of $\xi=2{,}300\ \mathrm{m}^{-2}$ and the same curvature radius as the experimental source are supposed. In both the vector diagrams, the length of arrow indicates the amplitude of each second harmonic component, and its angle from the dotted horizontal line expresses the phase parameter. Figure 6(b) well explains that the second harmonic components $P_{2\mathrm{I}}$ and $P_{2\mathrm{III}}$, which have been generated in the pre- and post-focal regions of the Gaussian source, cancel each other.[2] In contrast, the cancellation of $P_{2\mathrm{I}}$ and $P_{2\mathrm{III}}$ in Fig. 6(a) is less effective. Therefore the total second harmonic, which is the summation of $P_{2\mathrm{I}}+P_{2\mathrm{III}}$ shown by the arrow of broken lines and $P_{2\mathrm{II}}$, contains the components of $P_{2\mathrm{I}}+P_{2\mathrm{III}}$ more in the case of the present uniform source of Fig. 6(a). Further, in the present case, the quadrature component, whose phase parameter is $\pi/2$ rad, included in the total signal contains $P_{2\mathrm{I}}+P_{2\mathrm{III}}$ more. Even if fairly different values are assumed for s, a, d, and D, this situation still holds. Such a difference from Gaussian source is supposed to be caused by the edge of source. These behaviors of the second harmonic of the uniform source are disadvantageous to the B/A measurement because of less sensitivity to the own property of the sample. To increase the sensitivity, it is effective to employ much higher frequency which enhances the focusing gain. The high frequency, however, increases the attenuation, which is disadvantageous to the B/A measurement. Although a large aperture angle is effective to increase the focusing gain while keeping the frequency constant, an advanced analysis based on the model other than the KZK equation is necessary for such a sound source.

5. MEASUREMENT OF B/A

The determination of the B/A of sample was examined employing the experimental result for a methanol sample shown in Fig. 4. Equations (8) and (14) give the ratio of fundamental amplitudes $|P_{1s}/P_{1w}|$ observed at their maximum positions to be $T_{11}T_{01}\exp(-\alpha_1 L)$. Accordingly the measurement of the reduction of the fundamental amplitude due to the insertion of sample enables one to estimate α_1 when the values of T_{11}, T_{01} and L are known. Assuming the relation $\alpha_1/k \ll 1$ which holds for almost all the liquid samples, $T_{11}T_{01}$ can be evaluated from the density and sound speed in the sample and water; namely ρ_w, ρ, c_w, and c. On the other hand, the ratio of Eqs. (8) and (15) at each maximum range gives the theoretical value for the experimentally observed $|P_{2s}/P_{2w}|$, which increases linearly with the nonlinearity parameter of the sample, B/A. The calculated relation between $|P_{2s}/P_{2w}|$ and B/A of the methanol sample is shown in Fig. 7 for two cases of $\alpha_1=0$ and $\alpha_1=1.0$ Np/m, where the literature values for ρ and c as well as the assumption of $\alpha_2=4\alpha_1$ have been employed for the calculation. When $\alpha_1=0$ is assumed, the value of $|P_{2s}/P_{2w}|$ in this experiment, 2.7, leads to the B/A value of 9.9, which is close to the literature B/A value of 9.6. However, since the experimental observation of the fundamental amplitude reduction supports $\alpha_1=1.0$ Np/m, the result must be $B/A=10.8$, which is 13% larger than the literature value. The phase parameters Φ_w and Φ_s were never used in this determination, unlike the method employing the quantity named R_F defined for a Gaussian source.[8,9] The R_F is useful to selectively detect the second harmonic component generated within the sample, and to perform the experiment so that the influence of attenuation in the sample can be almost ignored. However the advantage of using such parameters has disappeared in the case of uniform source because the quadrature component in the second harmonic pressure does not correspond well to the component generated at the focal region as illustrated in Fig. 6. Then, the determination of B/A is much influenced by the attenuation coefficient of the sample unlike the case of using R_F. The uncertainty in estimation of the attenuation introduced by experimental setup and amplitude measurements, therefore, may give rise to a large measurement error

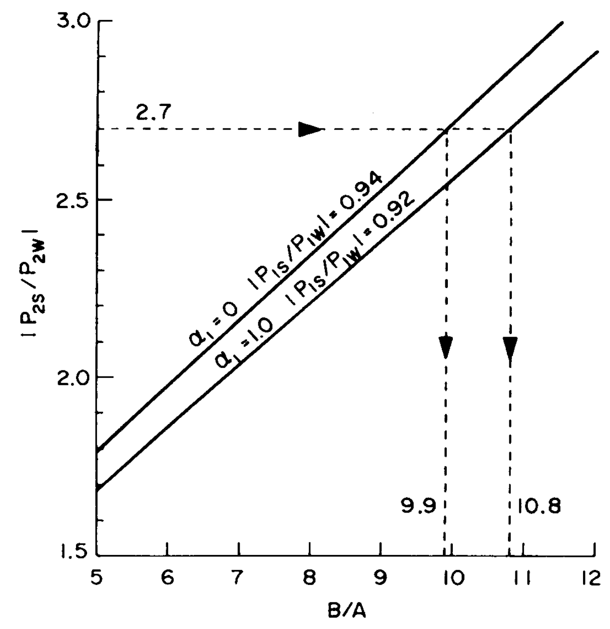

Fig. 7 Relation between $|P_{2s}/P_{2w}|$ and B/A for methanol sample.

Table 1 Comparison of measured and literature values of B/A.

Sample	This study	Literature
Methanol	10.8	9.6 (Ref. 12) 10.0 (Ref. 8)
Benzyl alcohol	9.1	10.2 (Ref. 12) 10.8 (Ref. 8)
n Butyl alcohol	12.8	10.7 (Ref. 12) 10.8 (Ref. 8)
Glycerin	8.5	8.8 (Ref. 13) 9.4 (Ref. 14) 9.3 (Ref. 8)

for the B/A. The result for methanol can be interpreted as a typical example for such inconvenient characteristics of the present determination method. Similar experiments were also conducted for other samples including benzyl alcohol, *n* butyl alcohol, and glycerin. Table 1 shows the comparison of the measured B/A with the literature values. The agreement is not good as was expected. The combination of uniform concave source and concave receiver, therefore, is assumed difficult to utilize for obtaining high precision in determining the B/A.

6. CONCLUSION

To realize the B/A measurement using an acoustic microscope, the property of nonlinearly generated second harmonic sound in a focused beam emitted by a uniformly excited concave source and detected by a concave receiver was investigated for both cases of free field and field with a sample inserted. Integrating the successive approximation solution of the KZK equation for the pressure over the concave receiver surface, the amplitudes and phase of the fundamental and second harmonic components of the receiver output can be derived. Since the present experimental receiver has a relatively large aperture, the approximation of infinite aperture radius also gives a valid estimate for the amplitude and phase of the received signal in the vicinity of the maximum amplitude range. Such sound properties as the range dependences of the fundamental and second harmonic amplitudes differing from each other, and the less effective cancellation of the second harmonic components generated at the pre- and post-focal regions, are different from the case of Gaussian source. These must be due to the influence of source-edge diffraction. When a different liquid layer is inserted, the influence of the nonlinearity parameter B/A of the sample evidently appears in the change of the second harmonic component observed beyond the sample, as predicted theoretically. The result of experimental determination of the B/A utilizing such responses, however, shows slightly poorer agreement with the literature values probably caused by the second harmonic component being less sensitive to the nonlinear property of the inserted sample.

ACKNOWLEDGMENTS

The author wishes to thank the members of the Nonlinear Acoustics Research Society for invaluable discussion. Messrs. Kazuyoshi Ono, Yoshiyuki Okada, and Manabu Kitamura are thanked for their assistance in the experiment. Mr. Thomas DeMary of The University of Texas at Austin is thanked for helping in revising the manuscript.

REFERENCES

1) S. Saito, B. C. Kim, and T. G. Muir, "Second harmonic component of a nonlinearly distorted wave in a focused sound field," J. Acoust. Soc. Am. **82**, 621-628 (1987).
2) S. Saito and B. C. Kim, "Selective detection of second harmonic sound generated at the focal region in a finite amplitude focusing field," J. Acoust. Soc. Jpn. (E) **8**, 165-175 (1987).
3) B. C. Kim and S. Saito, "Influence of inserted sample on second harmonic component in a finite-amplitude focused sound," J. Acoust. Soc. Jpn. (E) **10**, 143-151 (1989).
4) S. Saito and H. Tanaka, "Harmonic component of finite-amplitude sound in a focused Gaussian beam," J. Acoust. Soc. Jpn. (E) **11**, 225-233 (1990).
5) S. Saito and H. Tanaka, "Harmonic component of finite-amplitude sound in a focused Gaussian beam transmitting through a liquid layer," J. Acoust. Soc. Jpn. (E) **12**, 169-178 (1991).
6) S. Saito, "Second harmonic component of focused sound observed with a concave receiver," J. Acoust. Soc. Jpn. (E) **16**, 29-36 (1995).
7) W. K. Law, L. A. Frizzell, and F. Dunn, "Ultrasonic determination of the nonlinearity parameter B/A for biological media," J. Acoust. Soc. Am. **69**, 1210-1212 (1981).
8) S. Saito, "Measurement of the acoustic nonlinearity parameter in liquid media using focused ultrasound," J. Acoust. Soc. Am. **93**, 162-172 (1993).
9) S. Saito, "Measurement of acoustic nonlinearity parameter using focused ultrasound detected by a concave receiver," J. Acoust. Soc. Jpn. (E) **16**, 239-246 (1995).
10) B. G. Lucas and T. G. Muir, "The field of a focusing source," J. Acoust. Soc. Am. **72**, 1289-1296 (1982).
11) B. C. Kim, "Study on the analysis for second harmonic component of focused sound and the measurement of nonlinear property of the medium," Doctoral Thesis, Graduate School of Tokai University (1987), p. 66 (in Japanese).
12) R. T. Beyer, *Nonlinear Acoustics* (U. S. Naval Sea Systems Command, Washington, D. C., 1974), p. 101.
13) L. K. Zarembo and V. A. Krasil'nikov, "Some problems in the propagation of ultrasonic waves of finite amplitude in liquids," Sov. Phys. Usp. **2**, 580-599 (1959).
14) W. K. Law, L. A. Frizzell, and F. Dunn, "Determination of the nonlinearity parameter B/A for biological media," Ultrasound Med. Biol. **11**, 307-318 (1985).